Bioconjugate Chemistry

pubs.acs.org/bc

Article

Self-Assembling Nanoparticle Vaccines Displaying the Receptor Binding Domain of SARS-CoV-2 Elicit Robust Protective Immune Responses in Rhesus Monkeys

Heng Li,[¶] Lei Guo,[¶] Huiwen Zheng,[¶] Jing Li,[¶] Xin Zhao,[¶] Jiaqi Li, Yan Liang, Fengmei Yang, Yurong Zhao, Jinling Yang, Mengyi Xue, Yuanyuan Zuo, Jian Zhou, Yanli Chen, Zening Yang, Yanyan Li, Weihua Jin, Haijing Shi, Zhanlong He,[*,⊥] Qihan Li,[*,⊥] and Longding Liu[*,⊥]

Cite This: *Bioconjugate Chem.* 2021, 32, 1034−1046

Read Online

ACCESS | Metrics & More | Article Recommendations | Supporting Information

ABSTRACT: SARS-CoV-2 caused the COVID-19 pandemic that lasted for more than a year. Globally, there is an urgent need to use safe and effective vaccines for immunization to achieve comprehensive protection against SARS-CoV-2 infection. Focusing on developing a rapid vaccine platform with significant immunogenicity as well as broad and high protection efficiency, we designed a SARS-CoV-2 spike protein receptor-binding domain (RBD) displayed on self-assembled ferritin nanoparticles. In a 293i cells eukaryotic expression system, this candidate vaccine was prepared and purified. After rhesus monkeys are immunized with 20 μg of RBD−ferritin nanoparticles three times, the vaccine can elicit specific humoral immunity and T cell immune response, and the neutralizing antibodies can cross-neutralize four SARS-CoV-2 strains from different sources. In the challenge protection test, after nasal infection with 2×10^5 CCID50 SARS-CoV-2 virus, compared with unimmunized control animals, virus replication in the vaccine-immunized rhesus monkeys was significantly inhibited, and respiratory pathology observations also showed only slight pathological damage. These analyses will benefit the immunization program of the RBD−ferritin nanoparticle vaccine in the clinical trial design and the platform construction to present a specific antigen domain in the self-assembling nanoparticle in a short time to harvest stable, safe, and effective vaccine candidates for new SARS-CoV-2 isolates.

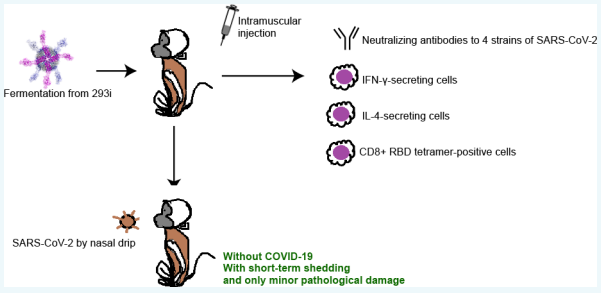

INTRODUCTION

Severe acute respiratory syndrome CoV-2 (SARS-CoV-2) causes coronavirus disease 2019 (COVID-19) and has remained a pandemic for more than a year. Among patients infected with SARS-COV-2, more than 80% have mild symptoms and good prognosis.[1] The fatality rate of SARS-CoV-2 was approximately 2.22%,[2] and it does not seem to be as high as those of SARS-CoV (9−11%) (8098 cases and 774 deaths)[3] or MERS (34%) (2494 cases and 858 deaths);[4] however, its transmission rate is substantially higher. The estimated mean R0 for COVID-19 is approximately 3.28;[5] consequently, SARS-CoV-2 has resulted in at least 112 456 453 confirmed cases and 2 497 514 deaths worldwide as of 26 February 2021.[2] Frustratingly, until now, few vaccines have been available to control the epidemic,[6] and strains with novel mutations arising in many areas pose great challenges to epidemic control and vaccine development.[7,8]

As of 23 February 2021, over 255 SARS-CoV-2 vaccine candidates were under development, including 73 in clinical trials (updated on 2021.2.23),[6] and some vaccine candidates were safe and could elicit immunity responses in the clinical trials.[9−15] Most vaccine candidates belong to one of five vaccine platforms: inactivated virus, DNA-based, viral vector, protein subunit, and RNA-based; several live attenuated virus vaccine candidates are also in development.[6] Of the active candidate vaccines in phase 3 trials, two are protein subunit vaccines, four are viral vector vaccines, one is a DNA-based vaccine, six are inactivated virus vaccines, and three are RNA-based vaccines.[6] It is encouraging that some vaccines[15−17] have shown more than 70%[16] and up to 95%[15] efficacy at preventing COVID-19, and these vaccines are now being used in many areas. However, the capacity to produce these vaccines is insufficient for worldwide administration, and more than half of the global population must receive a vaccine in order to contain the outbreak. In addition, concerns have emerged about poor vaccine stability in the field, security concerns about Pharmaceutical Process Scale-Up of the vaccine

Received: April 23, 2021
Revised: April 29, 2021
Published: May 6, 2021

https://doi.org/10.1021/acs.bioconjchem.1c00208
Bioconjugate Chem. 2021, 32, 1034−1046

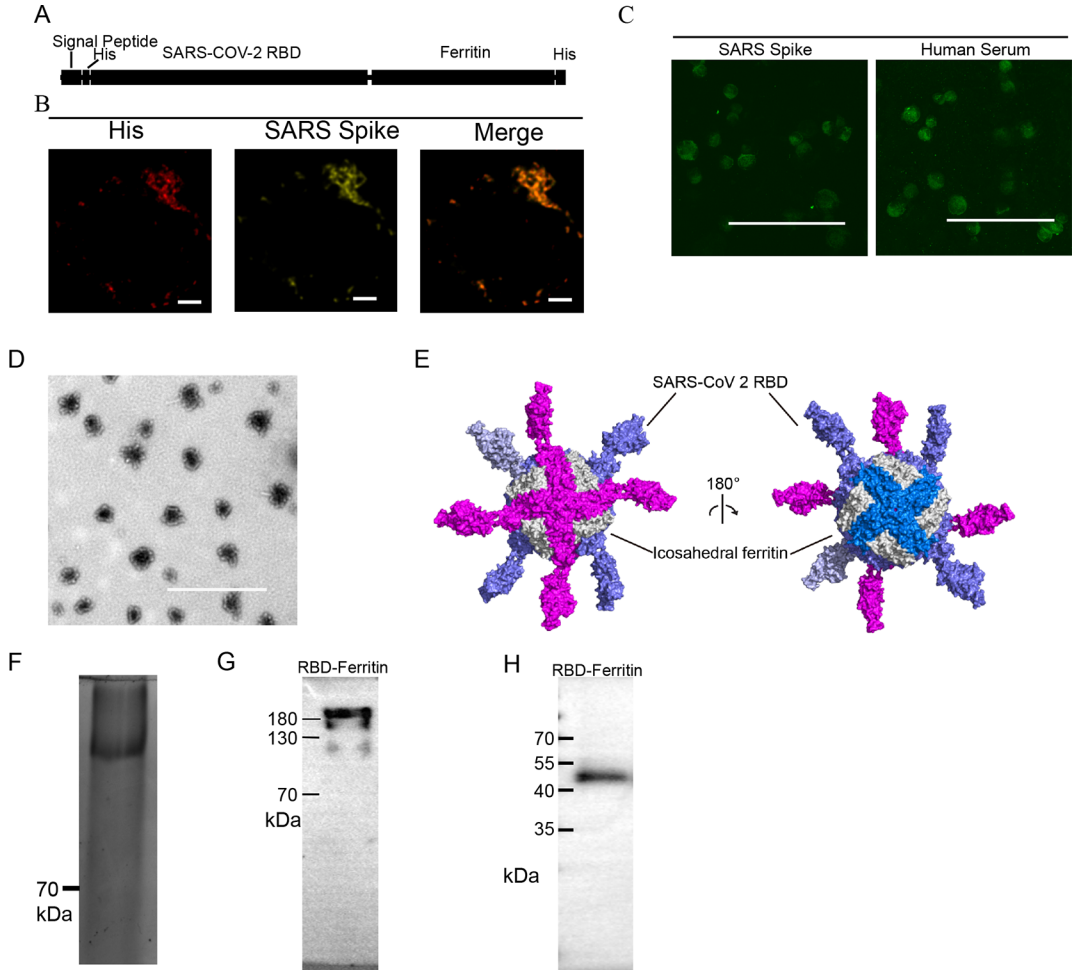

Figure 1. Ferritin-based self-assembling nanoparticles displaying the SARS-CoV-2 RBD. (A) Design of the RBD−ferritin fusion protein. (B) Immunofluorescence imaging of the RBD−ferritin fusion protein in 293T cells by His (red) and SARS spike antibody (green). The scale bar is 2 μm. (C) Immunofluorescent staining of the RBD−ferritin fusion protein in 293i cells by SARS spike antibody and convalescent human serum from infection by SARS-CoV-2. The scale bar is 125 μm. (D) TEM image of RBD−ferritin nanoparticles after affinity chromatography and supercentrifugation. The scale bar is 500 nm. (E) The homology model of the RBD−ferritin complex was predicted using SWISS-MODEL (https://swissmodel.expasy.org/). RBD and ferritin were generated by using the coordinates of the SARS-CoV-2 spike protein (PDB: 7CWS) and ferritin (PDB: 5C6F), respectively. The figures were prepared with PyMOL (http://www.pymol.org/). For clarity, eight RBDs fused to the ferritin monomers are shown. (F) The multimer of RBD−ferritin stained with Coomassie brilliant blue stain in native buffer. (G) Western blot of native PAGE showing multimeric RBD−ferritin extracted in native buffer, indicating an RBD−ferritin multimer of >180 kDa. (H) Western blot of M2e-ferritin extracted in denaturing buffer, indicating an RBD−ferritin fusion protein of ∼50 kDa.

production, and potentially weaker efficacy against isolates with mutations. It is therefore urgent to construct a universal, stable, effective vaccine platform for future vaccine development.

The SARS-CoV-2 virus relies on the spike protein in the viral membrane for host cell recognition, attachment, and membrane fusion. The receptor-binding domain (RBD) structure and sequence of SARS-CoV-2 and SARS are very similar, indicating a common origin.[18] However, the high hACE2 binding affinity of the RBD, furin preactivation of the spike protein, and hidden RBD in the spike potentially allow SARS-CoV-2 to maintain efficient cell entry while evading immune surveillance;[19−21] these may be the major reasons for its high transmission rate. Most of the isolated neutralizing antibodies against SARS-CoV-2 infection target the S protein,[22,23] especially the RBD.[23,24] Many vaccine candidates target the RBD, including several candidates in clinical trials.[6] Rapid conversion of recombinant RBD into particulate form via admixing with liposomes containing cobaltporphyrin-phospholipid (CoPoP) potently enhances the functional antibody response,[25] and this vaccine approach using RBD nanoparticles is now in phase I/II clinical trials (clinicaltrials.gov #NCT04783311).[6] A recombinant vaccine comprised of residues 319−545 of the RBD of the spike protein induced a potent functional antibody response in immunized mice, rabbits, and nonhuman primates (*Macaca mulatta*), and vaccination also provided protection against an in vivo challenge with SARS-CoV-2 in nonhuman primates.[26]

Self-assembling nanoparticle vaccine candidates with ferritin backbones can be conveniently and safely generated, and this platform has distinct advantages in terms of its relatively simple scale-up and flexible assembly. *Helicobacter pylori* (Hp) ferritin,[27,28] which self-assembles as a hollow spherical nanocage structure,[29] provides a good platform for RBD epitope presentation. Antigens associated with ferritin nanoparticles are more efficiently captured by DCs and macrophages than monomers.[30] Moreover, the heterogeneity of the nanoparticles may provide a self-adjuvant effect to elicit

https://doi.org/10.1021/acs.bioconjchem.1c00208
Bioconjugate Chem. 2021, 32, 1034−1046

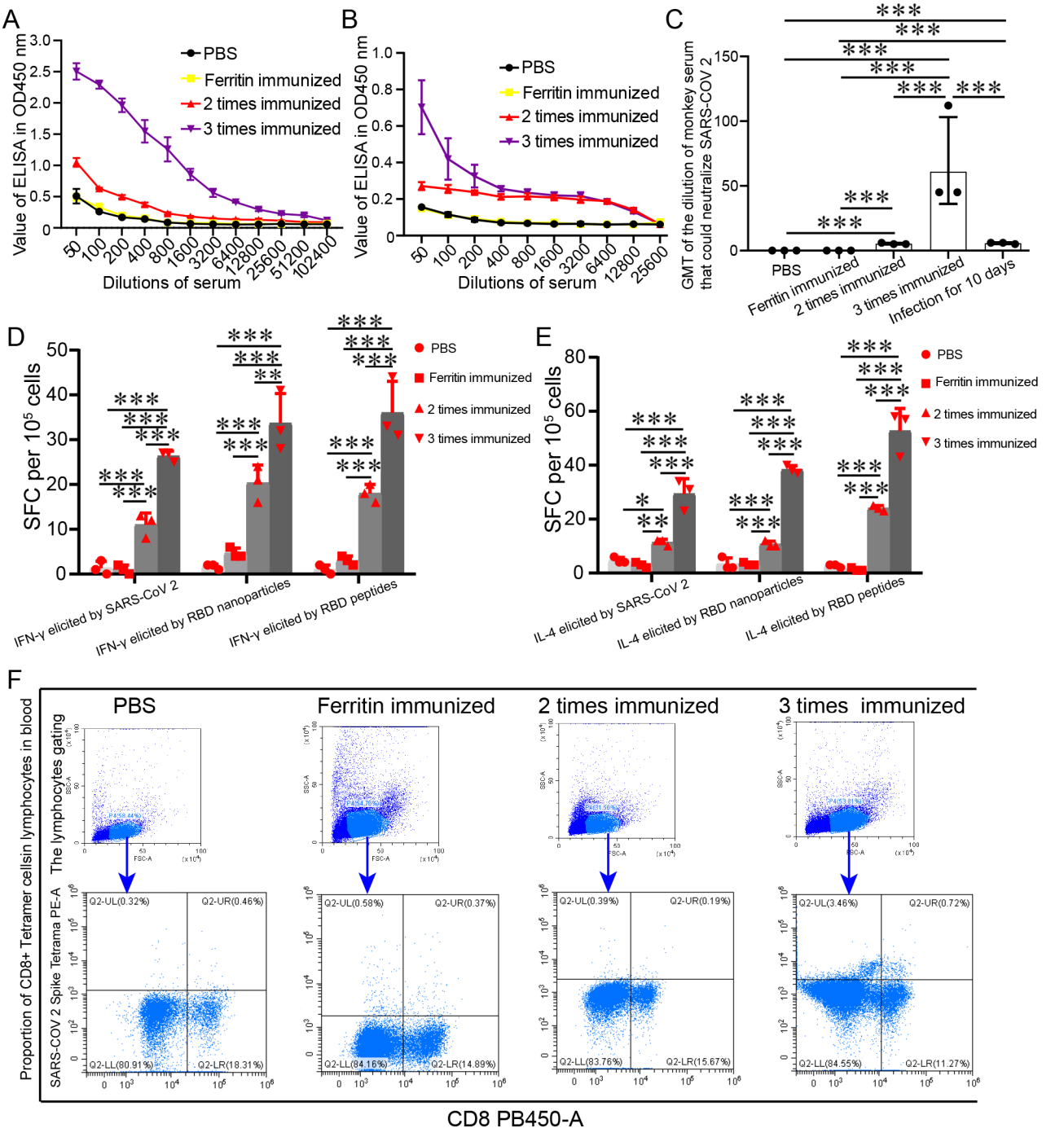

Figure 2. Humoral and T cell immune responses in RBD−ferritin nanoparticle-vaccinated rhesus monkeys. (A) The immune sera test for reactivity in an RBD nanoparticle-coating ELISA. $n = 3$ in every group. (B) The immune sera test for reactivity in an RBD peptide-coating ELISA, and the peptide was WNRKRISNCVAD. $n = 3$ in every group. (C) The neutralization ability of the serum was detected with 100 CCID50 SARS-CoV-2 from rhesus monkeys immunized two or three times with RBD nanoparticles and the monkeys infected with SARS-CoV-2 for 10 days. The cytopathic effect (CPE) was directly observed. The results were analyzed using GraphPad Prism 8, and p values were calculated by SPSS after the numbers of neutralization dilution were analyzed by log 10. $n = 3$ in every group. GMT in the y-axis is the geometric mean with geometric SD. (D, E) The SFCs of splenic lymphocytes secreting IFN-γ (D) and IL-4 (E) per 10^5 splenic lymphocytes in the immunized rhesus monkeys were evaluated via ELISPOT analysis after stimulation with 10^4 CCID50 SARS-CoV-2, 10 μg of RBD−ferritin nanoparticles, or 10 μg of RBD peptides including 2.5 μg of each peptide in four peptides belonging to the RBD. Peptide 1 was WNRKRISNCVAD, peptide 2 was GQTGKIADYNYK, peptide 3 was QAGSTPCNGVEG, and peptide 4 was GPKKSTNLVKNK, in order from the N-terminus to the C-terminus. $n = 3$ in every group. (F) CD8+ RBD tetramer-positive cells in PBMCs of immunized rhesus monkeys are shown. * $0.01 < P \leq 0.05$, ** $0.001 < P \leq 0.01$, *** $P \leq 0.001$.

immune responses without autoantibodies.[28] This platform has been successfully applied to influenza nanoparticle candidate vaccines.[27,31] Previous results showed that self-assembling nanoparticle vaccines displaying the RBD of SARS-CoV-2 could elicit robust immune responses in mice[30,32] and rhesus monkeys and protect against SARS-CoV-2 infection in hACE2

https://doi.org/10.1021/acs.bioconjchem.1c00208
Bioconjugate Chem. 2021, 32, 1034−1046

mice.[30] The antisera exhibited potent neutralizing activity and strong RBD competition with both ACE2 and neutralizing antibodies,[23] and strong CD8+ T cell and Th1-biased CD4+ T cell responses were induced in both mice and rhesus monkeys.[30] In addition, the RBD−ferritin nanoparticles had good stability.

To develop a SARS-CoV-2 vaccine platform with significant immunogenicity, high protection efficiency, broad spectrum, and good safety and to study the immune responses and protective effect of the RBD−ferritin nanoparticles in rhesus monkeys, we designed a self-assembling nanoparticle vaccine candidate and prepared it in an eukaryotic expression system (293i cells), followed by Ni-NTA purification and iodixanol ultracentrifugation to harvest RBD−ferritin nanoparticles. Then, rhesus monkeys were immunized with RBD−ferritin nanoparticles three times. The vaccine candidate elicited robust humoral and T cell responses, including cross-neutralization of four SARS-CoV-2 isolates; produced IFN-γ-secreting cells, IL-4-secreting cells, and specific CD8+ tetramer-expressing cells; and protected the rhesus monkeys from infection with 2×10^5 CCID50 SARS-CoV-2 with a short duration of shedding and slight pathological damage.

RESULTS

Construction and Purification of Self-Assembling Ferritin Nanoparticles Displaying SARS-CoV-2 RBD. The spike peptide sequences of four isolates of SARS-CoV-2 were compared, and we found that the RBD peptide was conserved (Figure S1B). The RBD peptide was fused to the N-terminus of ferritin, 6 × His was fused to the N-terminus of RBD, 10 × His was fused to the C-terminus of ferritin, and signal peptides were fused to the N-terminus of the RBD−ferritin fusion protein (Figure 1A). Immunofluorescence staining with His antibody and SARS spike antibody indicated the expression of the RBD−ferritin fusion protein in 293T cells after transfection with the recombinant plasmid (Figure 1B). Then, the expression of the RBD−ferritin fusion protein in 293i cells was validated with a SARS spike antibody (Figure 1C). Further, detection of the RBD−ferritin fusion protein expression with convalescent serum from human COVID-19 patients proved that the RBD−ferritin fusion protein could be recognized by the antibodies induced by SARS-CoV-2 infection (Figure 1C). The recombinant proteins were extracted in natural buffer and then purified by Ni-NTA and subsequent iodixanol supercentrifugation. We next observed the structural characteristics of the RBD−ferritin nanoparticles using negative staining electron microscopy. Transmission electron microscopy (TEM) images showed that the RBD−ferritin monomers could self-assemble into homogeneously sized nanoparticles (Figure 1D), and the homology model of the RBD−ferritin complex was predicted and is shown in Figure 1E. Native polyacrylamide gel electrophoresis (PAGE) and coomassie blue staining revealed a clear single band with a high molecular mass (Figure 1F). The RBD−ferritin fusion protein was further verified via Western blot analysis with the SARS spike antibody, and the results showed a specific single band of greater than 130 kDa on native PAGE (Figure 1G) and a specific single band of approximately 50 kDa on denaturing PAGE (Figure 1H). The theoretical mass of the RBD−ferritin fusion protein is 49.968 kDa. The purified RBD−ferritin nanoparticles were sequenced by mass spectrometry (MS), which also identified RBD−ferritin nanoparticles with correct sequences (Figure S2), and importantly, there was no other impurity protein in the results of MS.

Humoral and T Cell Immune Responses in RBD−Ferritin Nanoparticle-Vaccinated Rhesus Monkeys. RBD−ferritin nanoparticles (20 μg) were delivered by intramuscular injection at 2-week intervals, and serum and blood cell samples from the immunized rhesus monkeys were collected on the 28th days (immunized two times) and 42th days (immunized three times). The antigenicity of the RBD−ferritin nanoparticles was validated via Western blot analysis by SDS-PAGE using serum for antibody detection (Figure S3). We investigated the humoral immune responses after vaccination with RBD−ferritin nanoparticles. The test of immune sera for reactivity in an RBD-coating ELISA showed that the serum in the rhesus monkeys immunized three times with RBD−ferritin nanoparticles could bind to the RBD when the serum was diluted 102 400-fold, the serum in the rhesus monkeys immunized two times could bind to the RBD when the serum was diluted 25 600-fold, while the serum in the rhesus monkeys immunized with PBS or ferritin alone could bind when the serum was diluted 400-fold (Figure 2A). At the same time, the test of immune sera for reactivity in an RBD−peptide ELISA showed that the serum in the rhesus monkeys immunized two or three times with RBD−ferritin nanoparticles could bind to the RBD peptide when the serum was diluted 12 800-fold, while the serum in the rhesus monkeys immunized with PBS or ferritin alone could bind when the serum was diluted 50- to 100-fold (Figure 2B); thus, the serum in the rhesus monkeys immunized with RBD−ferritin nanoparticles three times had greater affinity for the RBD and peptide than those in the rhesus monkeys immunized with RBD−ferritin nanoparticles two times (Figure 2A, 2B). To evaluate whether the induced antibodies could neutralize authentic SARS-CoV-2, the neutralization capacity of serum from immunized rhesus monkeys was detected with 100 CCID50 SARS-CoV-2. Direct observation of the cytopathic effect (CPE) showed that the cells were not infected in the dilutions of 1/45 to 1/112 of the serum from the rhesus monkeys immunized three times, while the cells were not infected in the dilutions of 1/5 to 1/6 of the serum from the rhesus monkeys immunized two times (Figure 2C). In addition, we detected the convalescent sera neutralization level against SARS-CoV-2 using the serum from the monkeys on 10 dpi after SARS-CoV-2 infection and compared with the sera from the monkeys immunized with RBD, PBS, or ferritin nanoparticles. We found that the convalescent sera neutralization levels were lower obviously than those in the three times-immunized monkeys and similar to those in the two times-immunized monkeys (Figure 2C). At the same time, we found by ELISPOT and FLC that rhesus monkeys immunized with RBD−ferritin nanoparticles typically respond to vaccines with T cell-related immune effects (Figure 2D−F, Figure S4). The rhesus monkeys immunized with RBD−ferritin nanoparticles developed more IFN-γ-secreting cells and IL-4-secreting cells in their splenic lymphocytes, which were treated with 10 μg of RBD−ferritin fusion protein, 10 μg of RBD peptides, or 10^4 CCID50 SARS-CoV-2 as stimulants, and far more IFN-γ-secreting cells and IL-4-secreting cells were developed in the splenic lymphocytes from the rhesus monkeys that were immunized three times than those that were immunized only two times (Figure 2D, 2C). Equally importantly, CD8+ RBD tetramer-positive cells in PBMCs of immunized rhesus monkeys could be stimulated after three rounds of

https://doi.org/10.1021/acs.bioconjchem.1c00208
Bioconjugate Chem. 2021, 32, 1034−1046

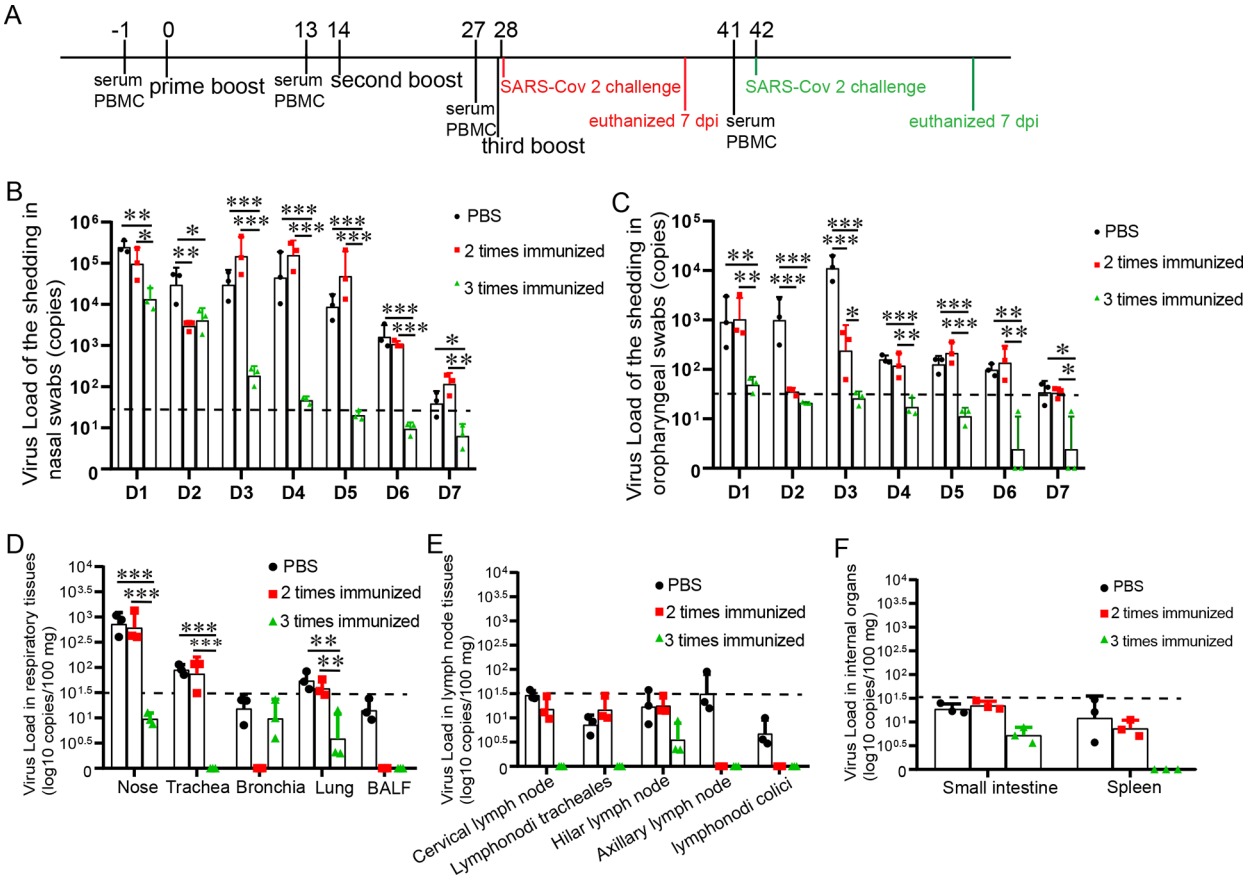

Figure 3. RBD−ferritin nanoparticles protected rhesus monkeys against SARS-CoV-2 challenge with low virus shedding and virus load. (A) Time points for immunization and sampling of rhesus monkeys. (B, C) SARS-CoV-2 shedding in the nose (B) and oropharynx (C) was detected in rhesus monkeys upon SARS-CoV-2 exposure for 7 days. $n = 3$ in every group. (D, E, F) The virus loads at 7 dpi in the respiratory tissues (D), lymph node tissues (E), and internal organs (F) of the rhesus monkeys upon SARS-CoV-2 exposure. $n = 3$ in every group. * $0.01 < P \leq 0.05$, ** $0.001 < P \leq 0.01$, *** $P \leq 0.001$.

immunization with RBD−ferritin nanoparticles, but not after only two rounds of immunization (Figure 2F). In summary, specific T cell responses could be stimulated after immunization with RBD−ferritin nanoparticles. In addition, lymphocyte responses were detected in immunized rhesus monkeys, and the proportions of CD3+ cells, CD4+ cells, CD8+ cells, CD4+ IFN γ+ cells, CD4+ IL-4+ cells, and CD4+ Foxp+ cells in lymphocytes in the blood after immunization with RBD−ferritin nanoparticles were increased, while the proportion of CD4+ IL-17+ cells in lymphocytes in the blood after immunization with RBD−ferritin nanoparticles was similar to that in rhesus monkeys immunized with PBS (Figure S4).

RBD−Ferritin Nanoparticles Protected Rhesus Monkeys against SARS-CoV-2 Challenge. RBD−ferritin nanoparticles could protect against SARS-CoV-2 infection in hACE2 mice after immunization two times;[30] however, RBD−ferritin nanoparticles could not protect rhesus monkeys after immunization two times. However, RBD−ferritin nanoparticles could protect against SARS-CoV-2 infection in rhesus monkeys after immunization three times (Figures 3, 4). These results will help to improve the RBD−ferritin nanoparticle vaccine immunization program chosen for clinical experiments. The rhesus monkeys immunized with RBD−ferritin nanoparticles three times were challenged with 2×10^5 CCID50 SARS-CoV-2. Rhesus monkeys immunized with ferritin protein only were not challenged because there was no positive immune response. The viral shedding in the nose, oropharynx, feces, and blood was monitored daily. The shedding viral load peaked at 3 and 4 dpi in the nose and oropharynx in rhesus monkeys immunized with PBS or immunized two times with RBD−ferritin nanoparticles, and the viral loads from the nasal swabs were higher than those from the oropharyngeal swabs. Encouragingly, there was little shedding at 3 dpi from the nose and below the limit of detection viral load from the oropharynx in the rhesus monkeys immunized with RBD−ferritin nanoparticles three times (Figure 3B, 3C). In addition, there was a below the limit of detection viral load in the feces or blood of any rhesus monkeys. Three rhesus monkeys from each group were sacrificed to allow the detection of the virus level, tissue damage, and immune responses at 7 dpi with SARS-CoV-2. There was no viral RNA in the respiratory tissues of the rhesus monkeys immunized three times with RBD−ferritin nanoparticles; at the same time, the viral RNA could be detected in the nose, and lesser virus RNA was detected in the lung, BALF, or trachea of the rhesus monkeys immunized with PBS or two rounds of RBD−ferritin nanoparticles (Figure 3D). IHC with SARS-CoV-2 N protein antibody showed that SARS-CoV-2 persisted in the lung and trachea in the rhesus monkeys immunized with PBS (Figure 4A, 4B). Similarly, IF with SARS-CoV-2 N protein antibody showed that SARS-CoV-2 persisted in the lung and trachea in the rhesus monkeys immunized with PBS or two rounds of RBD−ferritin nanoparticles (Figure 4C, 4D), but no SARS-CoV-2 was found in the lung and trachea in

https://doi.org/10.1021/acs.bioconjchem.1c00208
Bioconjugate Chem. 2021, 32, 1034−1046

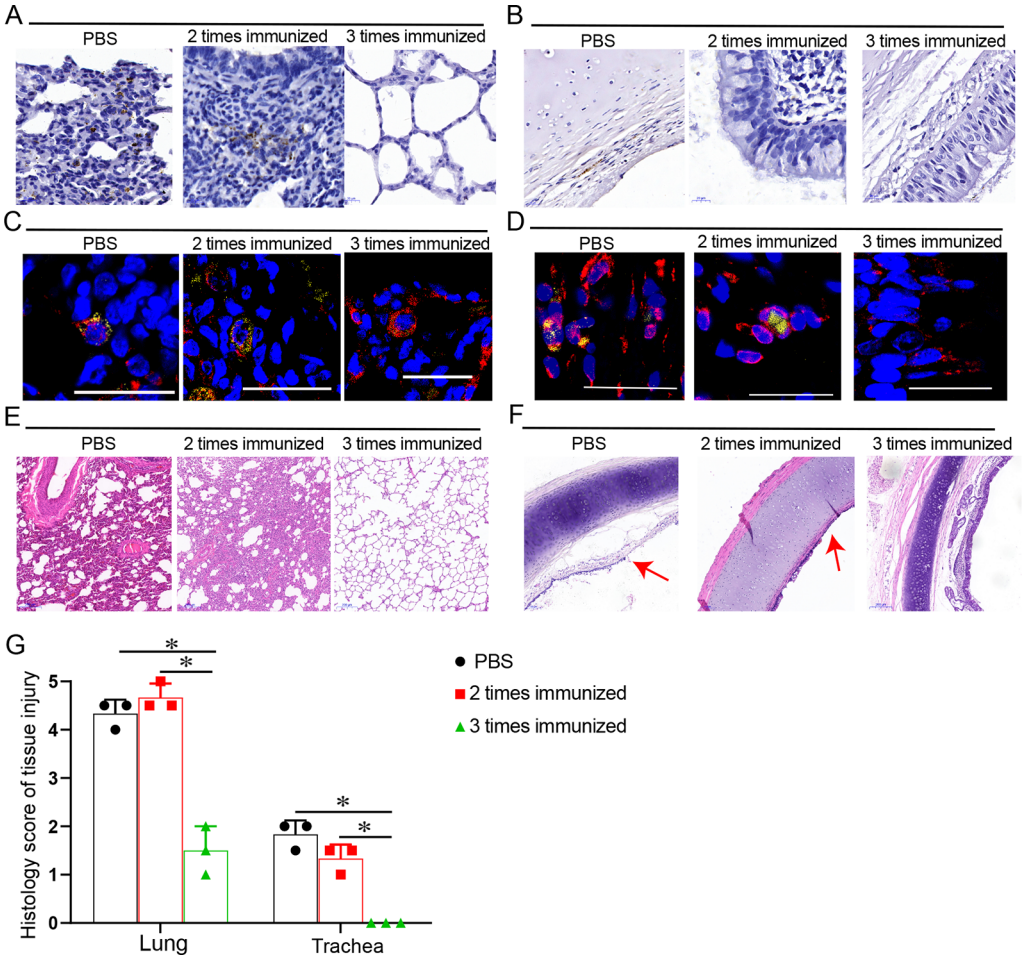

Figure 4. RBD−ferritin nanoparticles protected rhesus monkeys against SARS-CoV-2 challenge with little virus presence in the lung and trachea and slight pathological damage. (A, B) IHC with SARS-CoV-2 nucleocapsid antibody detected the virus in the lung (A) and trachea (B) of immunized rhesus monkeys. (C, D) IF with SARS-CoV-2 nucleocapsid antibody detected the virus in the lung (C) and trachea (D) of immunized rhesus monkeys. Red indicates ACE2; yellow indicates SARS-CoV-2. The scale bar is 30 μm. Lung (E) and tracheal (F) injury in immunized rhesus monkeys was detected by HE staining. The areas pointed to by the arrows in (F) are the injury points in the trachea. (G) Histology scores of lung and trachea were calculated according to the histology score standards in Tables S1 and S2. n = 3 in every group. The statistical analyses were calculated by Kruskal−Wallis analysis in SPSS. * $0.01 < P \leq 0.05$, ** $0.001 < P \leq 0.01$, *** $P \leq 0.001$.

the rhesus monkeys immunized with three rounds of RBD−ferritin nanoparticles (Figure 4A−D). There was little virus RNA in the lymph node tissues and internal organs in all rhesus monkeys (Figure 3E, 3F). In addition, the total protein concentration was obviously smaller in the BALF of the rhesus monkeys immunized with RBD−ferritin nanoparticles than those in the BALF of the rhesus monkeys immunized with PBS (Figure S5A). Cytospin analysis identified few cells in the BALF of the rhesus monkeys immunized with RBD−ferritin nanoparticles but many cells in the BALF of the rhesus monkeys immunized with PBS (Figure S5B, S5C).

After challenge with SARS-CoV-2 for 7 days, in the rhesus monkeys immunized with PBS, there were large areas of hemorrhage, some inflammatory cells infiltrated, and some alveolar septal cells thickened in the lung; local epithelial cells were exfoliated, and local hyperemia persisted in the trachea (Figure 4E, 4F). In the rhesus monkeys immunized two times with RBD−ferritin nanoparticles, many alveolar septal cells thickened, and inflammatory cells infiltrated the lung; local epithelial cells were exfoliated in the trachea (Figure 4E, 4F). In the rhesus monkeys immunized three times with RBD−ferritin nanoparticles, there was slight hyperplasia of local alveolar cells, and most cells in the lung and trachea were normal (Figure 4E, 4F). Histology scores of lung and trachea were calculated and also presented that there were few injuries in the lung and trachea in the monkeys immunized three times with RBD−ferritin nanoparticles (Figure 4G, Tables S1 and S2).

Lymphocyte Responses Were Also Suppressed in Immunized Rhesus Monkeys, While Specific CD8+ Tetramer Responses Were Maintained. Consistent with previous results,[1] T cell responses were suppressed in the SARS-CoV-2 infection process in all rhesus monkeys, including those immunized with RBD−ferritin nanoparticles (Figure 5, Figure S5D), but the CD4+ IFN-γ+ cells in the blood were more abundant at 3 dpi in the rhesus monkeys immunized with RBD−ferritin nanoparticles than in the rhesus monkeys immunized with PBS (Figure 5A), and there was perhaps a higher percentage of CD4+ IL-4+ cells in the blood at 1 dpi in the rhesus monkeys immunized with RBD−ferritin nanoparticles than in the rhesus monkeys immunized with PBS, but there was no statistical difference (Figure 5B); the CD4+ Foxp + cells in the blood from 0 to 3 dpi were greater in the rhesus monkeys immunized with RBD−ferritin nanoparticles than in

https://doi.org/10.1021/acs.bioconjchem.1c00208
Bioconjugate Chem. 2021, 32, 1034−1046

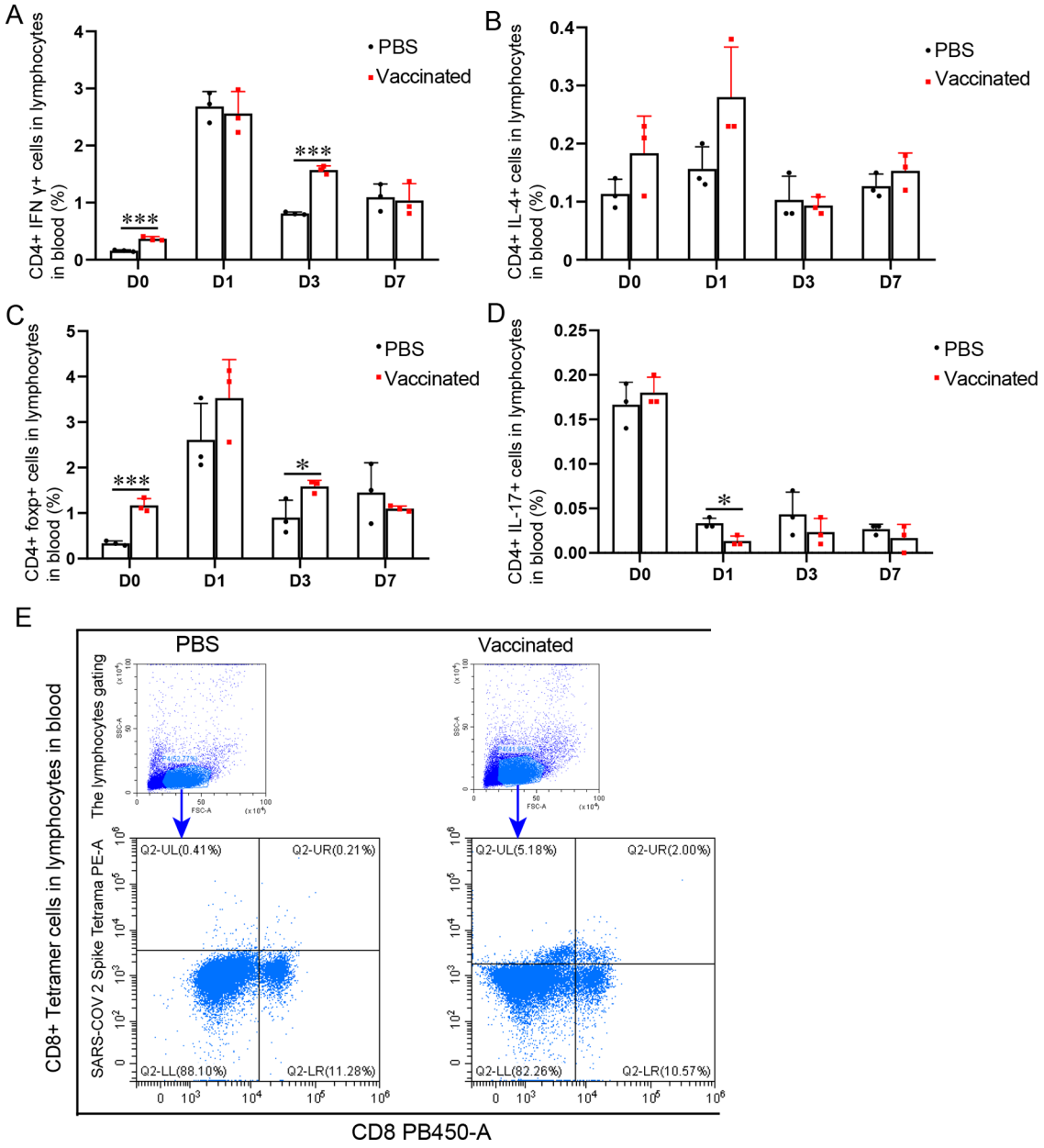

Figure 5. Lymphocyte responses were also suppressed in the immunized rhesus monkeys, while a specific CD8+ tetramer response was maintained. (A–D) CD4+ IFN-γ+ cell percentages (A), CD4+ IL-4+ cell percentages (B), CD4+ Foxp+ cells (C), and CD4+ IL-17+ cell percentages (D) in lymphocytes in the SARS-CoV-2 infection process were detected. $n = 3$ in every group. (E) CD8+ RBD tetramer-positive cells in lymphocytes in immunized rhesus monkeys at 7 dpi with SARS-CoV-2 infection are shown.

the rhesus monkeys immunized with PBS, but there was no statistical difference at 1 dpi (Figure 5C); in addition, neutrophil granulocytes were proliferative after infection with SARS-CoV-2, and they remained high over time in the rhesus monkeys immunized with RBD–ferritin nanoparticles (Figure S5E). More importantly, specific CD8+ tetramer responses were elicited after three immunizations with RBD–ferritin nanoparticles (Figure 2E), and proliferation was maintained throughout the SARS-CoV-2 infection (Figure 5E).

RBD–Ferritin Nanoparticles Can Elicit Universal Humoral Effects against Three Isolates of SARS-CoV-2 in Rhesus Monkeys. SARS-CoV-2 has remained epidemic among humans for over one year, and multiple mutations have arisen in many areas. Compared with SARS-CoV-2-KMS1/2020 (MT226610.1), there was no mutation in the RBD spike sequence in three other isolates (Figure S1B), but there was a K73N mutation in three isolates (Figure S1A), a D614G mutation in SARS-CoV-2/human/GBR/Kunming_kms-3/2020 and SARS-CoV-2/human/USA/Kunming_kms-6/2020 (Figure S1C), and an A828T mutation in SARS-CoV-2/human/KHM/Kunming_kms-2/2020 (Figure S1D). Here, cross-neutralization of serum of three times-immunized rhesus monkeys was detected for the other three isolates of SARS-CoV-2 from different sources. The cells were not infected in the dilutions of 1/22 to 1/27 of the serum from the rhesus monkeys immunized three times against 100 CCID50 SARS-CoV-2/human/KHM/Kunming_kms-2/2020, 1/45 to 1/74 against 100 CCID50 SARS-CoV-2/human/GBR/Kunming_kms-3/2020, and 1/14 to 1/45 against 100 CCID50 SARS-CoV-2/human/USA/Kunming_kms-6/2020, while the

https://doi.org/10.1021/acs.bioconjchem.1c00208
Bioconjugate Chem. 2021, 32, 1034–1046

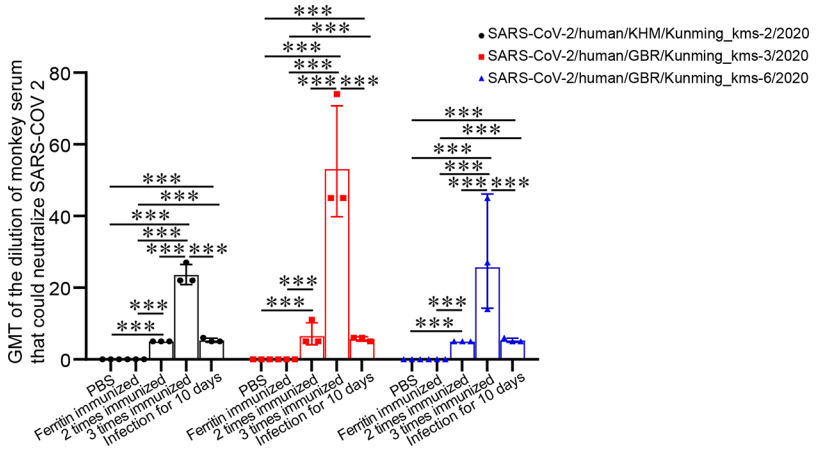

Figure 6. Cross-neutralization of the serum of immunized rhesus monkeys was detected with the other three isolates of SARS-CoV-2. The neutralization of the serum was detected for three other isolates of 100 CCID50 SARS-CoV-2 from rhesus monkeys immunized two or three times with RBD nanoparticles and the monkeys infected with SARS-CoV-2 for 10 days. The cytopathic effect (CPE) was directly observed. The three isolates of SARS-CoV-2 were SARS-CoV-2/human/KHM/Kunming_kms-2/2020 (MW341443.1), SARS-CoV-2/human/GBR/Kunming_kms-3/2020 (MW255832.1), and SARS-CoV-2/human/USA/Kunming_kms-6/2020 (MW264424.1). The results were analyzed using GraphPad Prism 8, and p values were calculated by SPSS after the numbers of neutralization dilution were analyzed by log 10. $n = 3$ in every group. GMT in the y-axis is the geometric mean with geometric SD * $0.01 < P \leq 0.05$, ** $0.001 < P \leq 0.01$, *** $P \leq 0.001$.

cells were not infected in the dilutions of 1/5 to 1/6 of the serum from the rhesus monkeys immunized two times or ones infected with SARS-CoV-2 at 10 dpi against 100 CCID50 SARS-CoV-2/human/KHM/Kunming_kms-2/2020, 1/5 to 1/11 against 100 CCID50 SARS-CoV-2/human/GBR/Kunming_kms-3/2020, and 1/5 against 100 CCID50 SARS-CoV-2/human/USA/Kunming_kms-6/2020 (Figure 6).

DISCUSSION

SARS-CoV-2 is the cause of a major pandemic, and immunization with safe and efficient vaccines to achieve full protection against SARS-CoV-2 infection is urgently needed. It is necessary to construct a universal, stable, effective vaccine platform for future vaccine development. Here, we prepared RBD−ferritin nanoparticles from an eukaryotic cell expression system (293i) and purified them by Ni-NTA and iodixanol ultracentrifugation. Importantly, the RBD−ferritin nanoparticles elicited potent immune responses, including humoral and T cell responses, and protected rhesus monkeys from infection by SARS-CoV-2 after three vaccinations. These analyses will benefit the immunization program of the RBD−ferritin nanoparticle vaccine in the clinical trial design and the platform construction to present a specific antigen domain in the self-assembling nanoparticle in a short time to harvest stable, safe, and effective vaccine candidates for new SARS-CoV-2 isolates. In addition, protein subunit vaccines utilize the RBD protein directly without requiring transcription or translation inside the human body to provide greater security.

Structural basis analysis of receptor recognition by SARS-CoV-2 found that SARS-CoV-2 RBDs are essential for ACE2 binding[18] and enhance its hACE2-binding affinity.[20] The position of the RBD on the spike protein 3D structure was analyzed by SWISS-MODEL (Figure S6), and the RBD was an independent domain in the spike protein; this would benefit the immunogenicity. Most of the isolated neutralizing antibodies against SARS-CoV-2 infection target the S protein,[22,23] especially the RBD.[23,24] Previous results showed that self-assembling nanoparticle vaccines displaying the RBD of SARS-CoV-2 elicited potent immune responses[30,32] and protected against SARS-CoV-2 infection in hACE2 mice after two vaccinations.[30] However, the protection efficiency of these nanoparticle vaccine candidates was limited in evaluation only in mice models. Considering that mice are not a suitable natural infecting model for SARS-CoV-2, the evaluation of vaccines in this model is limited because of the lack of the nonsystematic characteristics of the infection process. Based on the rhesus macaque model nasally inoculated with SARS-CoV-2, we think an evaluation on the protection of nanoparticle vaccines against SARS-CoV-2-infected nonhuman primates can provide more detailed data on the systemic immune response elicited by the vaccine. We harvested RBD−ferritin nanoparticles and administered them to rhesus monkeys at 20 μg per monkey. The results showed that three rounds of immunization with RBD−ferritin nanoparticles could protect rhesus monkeys from infection by 2×10^5 CCID50 SARS-CoV-2 with short-term shedding and only minor pathological damage, but the shedding after infection and lung and trachea damage were similar in the rhesus monkeys immunized with RBD−ferritin nanoparticles two times and those immunized with PBS.

COVID-19 has persisted as a worldwide epidemic for more than a year. One major concern is that several isolates with mutations have been found in patients, and thus we are facing the cocirculation of several isolates. These mutations include the D614G mutation in SARS-CoV-2/human/GBR/Kunming_kms-3/2020 and SARS-CoV-2/human/USA/Kunming_kms-6/2020 (Figure S1C) and N501Y and D570A mutations in SARS-CoV-2/human/ITA/APU-POLBA01/2020 (Figure S7). The D614G variant exhibits more efficient infection, replication, and competitive fitness in primary human airway epithelial cells but similar morphology and in vitro neutralization properties; the D614G variant also transmits significantly faster and displays increased competitive fitness in hamsters compared with the wild-type virus.[7] Fortunately, there is no mutation in the RBD sequence of the isolates with the D614G variant, and the RBD−ferritin nanoparticles therefore elicited universal humoral effects against the D614G variant (Figure 6). The N501Y and

https://doi.org/10.1021/acs.bioconjchem.1c00208
Bioconjugate Chem. 2021, 32, 1034−1046

D570A mutations occur in the RBD of SARS-CoV-2, and the isolate with the N501Y mutation was found to be more transmissible than the 501N lineage.[33] However, we did not evaluate cross-neutralization of this isolate. In other ways, cellular immune responses could also be involved in the clearance of virus infection. Strong CD8+ T cell and Th1-biased CD4+ T cell responses were induced in both mice and rhesus monkeys,[30] and in our results, strong T cell responses, including the presence of IFN-γ-secreting cells and IL-4-secreting cells, were also induced in rhesus monkeys after three immunizations. Interestingly, specific CD8+ tetramer cells were also induced in rhesus monkeys after three immunizations, and no SARS-CoV-2 isolates, including SARS-CoV-2/human/ITA/APU-POLBA01/2020, carry a mutation in the tetramer location. Therefore, it is possible that the immune responses elicited by our vaccine could protect against infection with these new SARS-CoV-2 isolates. In addition, ELISA with four peptides in the RBD showed that RBD−ferritin nanoparticles had the strongest binding with N-terminal peptides (Figure S8), which are not altered in these variants. Cross-neutralizing, specific CD8+ tetramer cells and universal IFN-γ-secreting cells, IL-4-secreting cells, TH1 cells, and Treg cells may play important roles in protection against infection by isolates with novel mutations. Of course, vaccines targeting isolates with mutations are necessary, and self-assembling nanoparticle platforms could be used to develop specific, stable, effective vaccines in a short time.

Self-assembling nanoparticle vaccines displaying the RBD of SARS-CoV-2 were prepared, and the vaccine candidate elicited robust humoral and T cell responses and protected the rhesus monkeys from infection by 2×10^5 CCID50 SARS-CoV-2 with short-term shedding and only minor pathological damage. These analyses will benefit the immunization program of the RBD−ferritin nanoparticle vaccine in the clinical trial design and the platform construction to present a specific antigen domain in the self-assembling nanoparticle in a short time to harvest stable, safe, and effective vaccine candidates for new SARS-CoV-2 isolates.

MATERIALS AND METHODS

Animals and Biosafety. All animal experiments were conducted under prior approval from the Animal Ethics Committee of the Institute of Medical Biology, IMBCAMS, permit number DWLL202004020, according to the National Guidelines on Animal Work in China. Twelve male rhesus macaques (age: 8−12 months; weight: 2−3 kg) were used in this study, and they come from IMBCAMS. All work with infectious SARS-CoV-2 was performed with approval under Biosafety Level 3 (BSL3) and Animal Biosafety Level 3 (ABSL3) conditions by the Institutional Biosafety Committee of Institute of Medical Biology (IMB) in the Kunming National High-level Biosafety Primate Research Center.

Viruses. The viral strain SARS-CoV-2-KMS1/2020 (GenBank accession number: MT226610.1) was isolated from sputum collected from a COVID-19 patient by the Chinese Academy of Medical Sciences (IMBCAMS) and propagated and tittered on Vero cells in DMEM (Sigma, USA). The three isolates of SARS-CoV-2 were SARS-CoV-2/human/KHM/Kunming_kms-2/2020 (MW341443.1), SARS-CoV-2/human/GBR/Kunming_kms-3/2020 (MW255832.1), and SARS-CoV-2/human/USA/Kunming_kms-6/2020 (MW264424.1) and were also isolated from sputum collected from the COVID-19 patients by the Chinese Academy of Medical Sciences (IMBCAMS) and propagated and tittered on Vero cells in DMEM (Sigma, USA). The stock viruses were frozen at −80 °C and prepared for the following experiments.

Plasmid Construction. A serine−glycine−glycine (Ser−Gly−Gly) spacer was fused to the gene fragment between the RBD from SARS-CoV-2-KMS1/2020 (GenBank accession number: MT226610.1) and ferritin. A signal peptide (ETDTLLLWVLLLWVPGSTGD) was fused in the N terminal of the fusion protein for secreting from 293i to the medium. Signal peptides−His−RBD−ferritin fusion genes were synthesized by TAKARA, and then the genes were cloned into pcDNA3.1(+) (Promega) vectors.

Protein Expression and Purification. To detect the expression of RBD−ferritin nanoparticles, expression vectors were transfected into 293T using the FuGENE HD transfection reagent (Promega) according to the manufacturer's instructions. The 293T cells were grown in DMEM with 2% FBS and then collected 2 days post-transfection. To produce ferritin and RBD−ferritin nanoparticles, expression vectors were transfected into the 293i cells using polyethyenimine (PEI) transfection reagent (Polysciences). 293i cells were grown in OPM-293 CD05 medium (Shanghai OPM Biosciences) with 37 °C, 8% CO_2, and 125 r/min, and the transfection conditions were 5×10^8 cells in 250 mL with 500 μg expression vectors and 1.5 mg of PEI; the cells were kept fermenting for 5 days at 37 °C, 8% CO_2, and 125 r/min.

The total proteins in the cells were extracted in their native forms by applying three freeze−thaw cycles, followed by ultrasonication at 40% strength for 6 s ON and 3 s OFF for 10 min. The nanoparticles were purified by affinity chromatography using Ni-NTA agarose (Invitrogen), and the total proteins were first incubated with Ni-NTA agarose at 4 °C for 2 h and washed in a gradient of 10, 20, and 40 mM imidazole until no protein was detected in the cleaning fluid, followed by elution in a gradient of 200 and 300 mM imidazole. Lastly, all the eluent was enriched using 10 K centrifugal filters. Iodixanol was prepared in 10-mL ultracentrifugation tubes with PBS-NaCl, and a continuous density gradient was produced from 6%−12%−18%−24%−30%−36%−42%−48%−54% iodixanol in 1 M NaCl. The proteins were flattened on the iodixanol followed by ultracentrifugation at 40 000 rpm for 4 h, and then the protein layer was collected. The nanoparticle proteins were dialyzed in a dialysis bag (MW: 12 000−14 000) in 2 mM PBS overnight and prepared for immunization.

Transmission Electron Microscopy (TEM) of RBD−Ferritin Nanoparticles. After purification by iodixanol supercentrifugation, the sampled layers containing nanoparticles were applied onto Formvar-carbon-coated 400-mesh copper grids using a glass microspray (Zhongjingkeyi, China). The grids were stained with 2% aqueous uranyl acetate at pH 4.5 for 5 min and viewed via a Hitachi TEM at 10 000−30 000× magnification.

Characterization of the RBD−Ferritin Nanoparticles. The protein purity and size were verified by native-PAGE-coomassius bright blue stain and SDS-PAGE-Western blot, and the primary antibody was the SARS spike antibody (Sino Biological, China). The mass spectrum of the fusion protein was detected by the Sangon, in Shanghai.

Animal Immunity and Viral Challenge. Six rhesus monkeys were immunized intramuscularly with 20 μg of RBD−ferritin nanoparticles with a 50% (v/v) mixture of aluminum adjuvant (Sigma), and three of the six monkeys were immunized two times while three of the six monkeys were

https://doi.org/10.1021/acs.bioconjchem.1c00208
Bioconjugate Chem. 2021, 32, 1034−1046

immunized three times. Three rhesus monkeys were immunized intramuscularly with 20 μg of ferritin nanoparticles with a 50% (v/v) mixture of aluminum adjuvant (Sigma) three times, and three rhesus monkeys were immunized intramuscularly with PBS with a 50% (v/v) mixture of aluminum adjuvant (Sigma) three times. Three rhesus monkeys were challenged by 2×10^5 CCID50 SAR-CoV 2 2 weeks after the second immunization, and three rhesus monkeys were challenged by 2×10^5 CCID50 SAR-CoV-2 2 weeks after the third immunization. The shedding in the nose, oropharynx, fecal matter, and blood were monitored every day after infection.

ELISA. Four RBD peptides (peptide 1 was WNRKRISNCVAD, peptide 2 was GQTGKIADYNYK, peptide 3 was QAGSTPCNGVEG, and peptide 4 was GPKKSTNLVKNK), synthesized at Syn (Nanjing, Jiangsu, China) with a purity above 98%, were diluted to 5 μg/mL and coated onto a plate at 100 μL/well, followed by incubation overnight at 4 °C, and a gradient dilution of serum samples was added to the plate for 1 h at 37 °C after blocking for 2 h. Then, monkey anti-IgG was added for 1 h at 37 °C, TMB was then added to develop color, and the data were detected at OD450 after a termination reaction.

ELISPOT. The spot-forming cells (SFCs) of IFN-γ-secreting cells and IL-4-secreting cells after antigen stimulation were evaluated using ELISPOT Kits (Mabtech) according to the manufacturer's instructions. In brief, 2 weeks after the second and third immunization, the monkeys splenic lymphocytes were isolated and plated in a 96-well membrane plate at 1×10^5 cells, followed by stimulation with 10 μg of RBD−ferritin nanoparticles, 10 μg of RBD peptides (with 2.5 μg of each RBD peptide 1−4), or 10^4 CCID50 SARS-CoV-2. The cells with stimulates were incubated at 37 °C under 5% CO_2 for 36 h. The number of spots was counted with an ImmunoSpot image analyzer (AID).

Neutralization Assay. Neutralization was measured in a formally validated assay that utilized four isolates of SARS-CoV-2 including SARS-CoV-2-KMS1/2020, SARS-CoV-2/human/KHM/Kunming_kms-2/2020, SARS-CoV-2/human/GBR/Kunming_kms-3/2020, and SARS-CoV-2/human/USA/Kunming_kms-6/2020. First 100 CCID50 virus in 50 μL per well was incubated with 12 serial twofold dilutions of serum samples in 50 μL per well in duplicate for 1 h at 37 °C in 96-well plates, and four parallelism wells were conducted. Cells were detached using 0.25% trypsin (Sigma), suspended in growth medium (100 000 cells/mL), and immediately added to all wells (10 000 cells in 100 μL of growth medium per well). One set of 12 wells received cells + virus (virus control), another set of 12 wells received cells only (background control), and another set of 12 wells received cells + serum without dilution (serum control). After 5−7 days of incubation, the neutralization assay could be judged according to CPE. Serum samples were heat-inactivated for 30 min at 56 °C prior to assay. The neutralization assays were calculated according to the Reed−Muench method.

Virus Load Detection. RNA from oropharyngeal swabs, nasal swabs, feces swabs, whole blood, and homogenized tissues was extracted using TRIzol reagent (Tiangen, China). The primers and probe used were ORF1ab-F: 5′-CCCTGTGGGTTTTACACTTA-3′; ORF1ab-R: 5′-ACGATTGTGCATCAGCTG-3′, and ORF1ab-P: 5′-CCGTCTGCGGTATGTGGAAAGGTTATGG-3′. For quantitation of viral RNA, a standard curve was generated using 10-fold dilutions of RNA standard; the standard curve was $y = -0.3052x + 11.444$. qRT-PCR was performed using a TaqMan Gene Expression Kit (Takara, China).

Histopathology. The specimens were fixed in 10% formalin for more than 1 week, and then the samples were fixed in 10% formalin for 2 h, 1 h in 70% ethanol, 1 h in 80% ethanol, 1 h in 90% ethanol, 1 h in 95% ethanol for three times, 1 h in xylene, 30 min in xylene, 30 min in paraffin, and 1 h in paraffin for two times. After slicing, the sections of paraffin-embedded tissue were deparaffinized in xylene, rehydrated in a graded series of ethanol, and rinsed with double-distilled water and then hematoxylin for 15 min, water for 1 min, 1% HCl in ethanol for 5 s, water for 1 min, ammonium hydroxide for 10 s, water for 1 min, 0.5% eosin for 30 s, 75% ethanol for 10 s, 95% ethanol for 10 s for two times, ethanol for 10 s for two times, and xylene for 10 s for two times.

Immunohistochemistry (IHC). The sections of paraffin-embedded tissue were deparaffinized in xylene, rehydrated in a graded series of ethanol, and rinsed with double-distilled water. The sections were incubated with rabbit anti-N antigen of SARS-CoV-2 (Sino Biological, China) for 1 h after heat-induced epitope retrieval. Antibody labeling was visualized by the development of DAB. Digital images were captured and evaluated by a histological section scanner (Aperio Digital Pathology, Leica).

Immunofluorescence (IF). Paraffin-embedded tissue sections were dewaxed, antigen repair was performed, and the tissue sections were blocked for 1 h in 5% BSA at room temperature and then labeled with an anti-ACE2 antibody (Abcam, ab15348) at a 1:500 dilution overnight at 4 °C. The tissue slides were permeabilized with 0.1% Triton X-100 for 15 min and then anti-SARS-CoV-2 N protein antibody (Sino Biological, China) at a 1:500 dilution for 1 h at room temperature. Finally, SARS-CoV-2 N protein antigens were visualized by Alexa Fluor 555-conjugated donkey antimouse IgG (Invitrogen) at a 1:500 dilution, and ACE2 protein antigens were visualized by Alexa Fluor 647-conjugated donkey anti-rabbit IgG (Invitrogen) at a 1:500 dilution for 1 h. The images were captured by a Leica TCS SP8 laser confocal microscope.

Immunophenotyping. The number of lymphocytes was detected by CD3 (FITC-conjugate), CD4 (PE-conjugate), CD8 (APC-conjugate), IFN-γ (BV421-conjugated), FOXP-3 (FITC-conjugated), IL-4 (PC7-conjugated), IL-17 (APC-conjugated) staining, and RBD tetramer (PE-conjugate). All of these antibodies were purchased from BD Biosciences, USA. The RBD tetramer location was YFPLQSYGF, and they were purchased from Creative Biosciences. Red blood cells were lysed using BD Pharm Lyse. The cells were permeabilized using BD permeabilization/fixation reagent. The cells were resuspended in 0.2 mL of 2% paraformaldehyde until they were run on a Beckman flow cytometer. Flow cytometry data were analyzed using CytoFLEX (BECKMAN).

Statistical Analysis. The data were analyzed and plotted using GraphPad Prism 8, and p values were calculated by one-way ANOVA using SPSS PASW statistical software version 18.0. p values in Figure 4G were calculated by Kruskal−Wallis analysis. * $0.01 < P \leq 0.05$, ** $0.001 < P \leq 0.01$, and *** $P \leq 0.001$.

https://doi.org/10.1021/acs.bioconjchem.1c00208
Bioconjugate Chem. 2021, 32, 1034−1046

■ ASSOCIATED CONTENT

Supporting Information

The Supporting Information is available free of charge at https://pubs.acs.org/doi/10.1021/acs.bioconjchem.1c00208.

Spike sequence comparison among four isolates of SARS-CoV-2; RBD−ferritin fusion protein sequenced by mass spectrometry; antigenicity of the RBD−ferritin nanoparticles validated via Western blot analysis; lymphocyte response detection in immunized rhesus monkeys; immune responses in the rhesus monkeys infected with SARS-CoV-2; the position of the RBD on the spike protein 3D structure; RBD sequence comparison among five isolates of SARS-CoV-2; ELISA of RBD−ferritin nanoparticles with four peptides in the RBD; histology score standards of lung damage; histology score standards of trachea damage (PDF)

■ AUTHOR INFORMATION

Corresponding Authors

Longding Liu − *Institute of Medical Biology, Chinese Academy of Medical Sciences & Peking Union Medical College, Kunming 650118, China; Key Laboratory of Systemic Innovative Research on Virus Vaccine, Chinese Academy of Medical Sciences, Kunming 650118, China*; Phone: 86-871-68335905; Email: longdingl@gmail.com; Fax: 86-871-68334483

Qihan Li − *Institute of Medical Biology, Chinese Academy of Medical Sciences & Peking Union Medical College, Kunming 650118, China*; Email: liqihan@imbcams.com.cn

Zhanlong He − *Institute of Medical Biology, Chinese Academy of Medical Sciences & Peking Union Medical College, Kunming 650118, China*; Email: hzl@imbcams.com.cn

Authors

Heng Li − *Institute of Medical Biology, Chinese Academy of Medical Sciences & Peking Union Medical College, Kunming 650118, China; Key Laboratory of Systemic Innovative Research on Virus Vaccine, Chinese Academy of Medical Sciences, Kunming 650118, China*; orcid.org/0000-0002-6352-2469

Lei Guo − *Institute of Medical Biology, Chinese Academy of Medical Sciences & Peking Union Medical College, Kunming 650118, China; Key Laboratory of Systemic Innovative Research on Virus Vaccine, Chinese Academy of Medical Sciences, Kunming 650118, China*

Huiwen Zheng − *Institute of Medical Biology, Chinese Academy of Medical Sciences & Peking Union Medical College, Kunming 650118, China; Key Laboratory of Systemic Innovative Research on Virus Vaccine, Chinese Academy of Medical Sciences, Kunming 650118, China*

Jing Li − *Institute of Medical Biology, Chinese Academy of Medical Sciences & Peking Union Medical College, Kunming 650118, China*

Xin Zhao − *Institute of Medical Biology, Chinese Academy of Medical Sciences & Peking Union Medical College, Kunming 650118, China; Key Laboratory of Systemic Innovative Research on Virus Vaccine, Chinese Academy of Medical Sciences, Kunming 650118, China*

Jiaqi Li − *Trinomab Biotech Co., Ltd., Zhuhai 519090, China*

Yan Liang − *Institute of Medical Biology, Chinese Academy of Medical Sciences & Peking Union Medical College, Kunming 650118, China*

Fengmei Yang − *Institute of Medical Biology, Chinese Academy of Medical Sciences & Peking Union Medical College, Kunming 650118, China*

Yurong Zhao − *Institute of Medical Biology, Chinese Academy of Medical Sciences & Peking Union Medical College, Kunming 650118, China*

Jinling Yang − *Institute of Medical Biology, Chinese Academy of Medical Sciences & Peking Union Medical College, Kunming 650118, China*

Mengyi Xue − *Institute of Medical Biology, Chinese Academy of Medical Sciences & Peking Union Medical College, Kunming 650118, China*

Yuanyuan Zuo − *Institute of Medical Biology, Chinese Academy of Medical Sciences & Peking Union Medical College, Kunming 650118, China*

Jian Zhou − *Institute of Medical Biology, Chinese Academy of Medical Sciences & Peking Union Medical College, Kunming 650118, China*

Yanli Chen − *Institute of Medical Biology, Chinese Academy of Medical Sciences & Peking Union Medical College, Kunming 650118, China*

Zening Yang − *Institute of Medical Biology, Chinese Academy of Medical Sciences & Peking Union Medical College, Kunming 650118, China*

Yanyan Li − *Institute of Medical Biology, Chinese Academy of Medical Sciences & Peking Union Medical College, Kunming 650118, China*

Weihua Jin − *Institute of Medical Biology, Chinese Academy of Medical Sciences & Peking Union Medical College, Kunming 650118, China*

Haijing Shi − *Institute of Medical Biology, Chinese Academy of Medical Sciences & Peking Union Medical College, Kunming 650118, China; Key Laboratory of Systemic Innovative Research on Virus Vaccine, Chinese Academy of Medical Sciences, Kunming 650118, China*

Complete contact information is available at: https://pubs.acs.org/10.1021/acs.bioconjchem.1c00208

Author Contributions

¶These authors contributed equally to this work.

Author Contributions

⊥These authors also contributed equally to this work.

Author Contributions

L.D.L. and Q.H.L. designed the studies. L.D.L. and H.L. analyzed the data and prepared and wrote the manuscript. H.L, L.G., and X.Z. performed the experiments. H.W.Z. and J.L. conducted the virologic assays. J.Q.L. performed the cell fermentation experiments. Y.L., FM.Y., YR.Z., MY.X., and ZL.H. conducted the rhesus macaques studies and performed the virus loads detection. JL.Y. participated in histopathology experiments. YY.Z., J.Z., YL.C., ZN.Y., YY.L., W.H.J., and H.J.S. participated in discussions and manuscript preparation. All the authors discussed the results and commented on the manuscript.

Funding

Funding was provided by the National Natural Science Foundation of China (32070923; 82041017); CAMS Innovation Fund for Medical Sciences (2020-I2M-2−014); the Yunnan Applied Basic Research Projects (2018FB113).

Notes

The authors declare no competing financial interest.

Data Sharing. All the data generated or analyzed during this study are included in this published article, and the additional files are available from the corresponding author upon reasonable request.

■ ACKNOWLEDGMENTS

We thank the Kunming National High-level Biosafety Primate Research Center for its support.

■ REFERENCES

(1) Chen, N., Zhou, M., Dong, X., Qu, J., Gong, F., Han, Y., Qiu, Y., Wang, J., Liu, Y., Wei, Y., et al. (2020) Epidemiological and clinical characteristics of 99 cases of 2019 novel coronavirus pneumonia in Wuhan, China: a descriptive study. *Lancet 395* (10223), 507−513.

(2) WHO Coronavirus Disease (COVID-19) Dashboard. https://covid19.who.int/table.

(3) Centers for Disease Control and Prevention. Frequently asked questions about SARS. 2005. https://www.cdc.gov/sars/about/faq.html.

(4) World Health Organization. Middle East respiratory syndrome coronavirus (MERS-CoV). https://www.who.int/emergencies/mers-cov/en.

(5) Liu, Y., Gayle, A., Wilder-Smith, A., and Rocklöv, J. (2020) The reproductive number of COVID-19 is higher compared to SARS coronavirus. *J. Travel Med. 27* (2), taaa021.

(6) Draft landscape and tracker of COVID-19 candidate vaccines. https://www.who.int/publications/m/item/draft-landscape-of-covid-19-candidate-vaccines?__cf_chl_captcha_tk__=059a275a2e7ff9e37a9c10919293f6a43d69eab6-1614344806-0-ARnagPnEq8IwLtOWgBykquVkCTUnHctVszshgc8QfauUoTY_-kv0aSnkVQyd4bfajCCEg1uAdh1uITGShxJ0sWLEgr7kR6OOHGdVyZthq7gvT8s5MYOEFG-i1JXI8B_5_mIVb02_71ByOaXymZYhNcyEu_t9U9v9sgxUdJ4WDZ-yyQgpG--0xKmNABHMjjJ9vGIfpKPou9nHWN5eToUdPn6SzSpdh_EhzBQa3Txs9ZIStCTvLV6YJ7mgzqL9phygEqiuhMrCrvornouOJHL09p8BcxEv2osJFZGIzd1eFj1A-yCzUXsgF_nK7mibVl1jsfc3AU9_21Hj8Ru6sj7GzNMpdJMGpWolV7Vfbhak1MbL49Wrx1przFds0HX0NwJVunfeULWflaUOC-Cpcgscu50bj8-7BT3uRHaA0s1tIJI2km_G4-3MTIEkoLhVRswrCHXkjh1d5VJBgKHycg1SjcWN7D3t0Luno3xrPUiizRXeU_BtcH6TgIKUYR7MCL1j8H1t0RhOoK2tiJX7vFLKyO48CMIwr1M6V7JaN-S_FuMoZvia_YXMcSGg1Z7gOZThCTGIGHCGgIv3QUMWWMKpqXzIU9dFA4rjBE51i4XJOumP-SzKNrihISfIYgfxVCGqFg.

(7) Hou, Y. J., Chiba, S., Halfmann, P., Ehre, C., Kuroda, M., Dinnon, K. H., 3rd, Leist, S. R., Schafer, A., Nakajima, N., Takahashi, K., et al. (2020) SARS-CoV-2 D614G variant exhibits efficient replication ex vivo and transmission in vivo. *Science 370* (6523), 1464−1468.

(8) Leung, K., Shum, M. H., Leung, G. M., Lam, T. T., and Wu, J. T. (2021) Early transmissibility assessment of the N501Y mutant strains of SARS-CoV-2 in the United Kingdom, October to November 2020. *Euro Surveill 26* (1), 2002106.

(9) Folegatti, P. M., Ewer, K. J., Aley, P. K., Angus, B., Becker, S., Belij-Rammerstorfer, S., Bellamy, D., Bibi, S., Bittaye, M., Clutterbuck, E. A., et al. (2020) Safety and immunogenicity of the ChAdOx1 nCoV-19 vaccine against SARS-CoV-2: a preliminary report of a phase 1/2, single-blind, randomised controlled trial. *Lancet 396* (10249), 467−478.

(10) Xia, S., Zhang, Y., Wang, Y., Wang, H., Yang, Y., Gao, G. F., Tan, W., Wu, G., Xu, M., Lou, Z., et al. (2021) Safety and immunogenicity of an inactivated SARS-CoV-2 vaccine, BBIBP-CorV: a randomised, double-blind, placebo-controlled, phase 1/2 trial. *Lancet Infect. Dis. 21* (1), 39−51.

(11) Iqbal Yatoo, M., Hamid, Z., Parray, O. R., Wani, A. H., Ul Haq, A., Saxena, A., Patel, S. K., Pathak, M., Tiwari, R., Malik, Y. S., et al. (2020) COVID-19 - Recent advancements in identifying novel vaccine candidates and current status of upcoming SARS-CoV-2 vaccines. *Hum. Vaccines Immunother. 16* (12), 2891−2904.

(12) Widge, A. T., Rouphael, N. G., Jackson, L. A., Anderson, E. J., Roberts, P. C., Makhene, M., Chappell, J. D., Denison, M. R., Stevens, L. J., Pruijssers, A. J., et al. (2021) Durability of Responses after SARS-CoV-2 mRNA-1273 Vaccination. *N. Engl. J. Med. 384* (1), 80−82.

(13) Keech, C., Albert, G., Cho, I., Robertson, A., Reed, P., Neal, S., Plested, J. S., Zhu, M., Cloney-Clark, S., Zhou, H., et al. (2020) Phase 1−2 Trial of a SARS-CoV-2 Recombinant Spike Protein Nanoparticle Vaccine. *N. Engl. J. Med. 383* (24), 2320−2332.

(14) Anderson, E. J., Rouphael, N. G., Widge, A. T., Jackson, L. A., Roberts, P. C., Makhene, M., Chappell, J. D., Denison, M. R., Stevens, L. J., Pruijssers, A. J., et al. (2020) Safety and Immunogenicity of SARS-CoV-2 mRNA-1273 Vaccine in Older Adults. *N. Engl. J. Med. 383* (25), 2427−2438.

(15) Polack, F. P., Thomas, S. J., Kitchin, N., Absalon, J., Gurtman, A., Lockhart, S., Perez, J. L., Perez Marc, G., Moreira, E. D., Zerbini, C., et al. (2020) Safety and Efficacy of the BNT162b2 mRNA Covid-19 Vaccine. *N. Engl. J. Med. 383* (27), 2603−2615.

(16) Voysey, M., Clemens, S. A. C., Madhi, S. A., Weckx, L. Y., Folegatti, P. M., Aley, P. K., Angus, B., Baillie, V. L., Barnabas, S. L., Bhorat, Q. E., et al. (2021) Safety and efficacy of the ChAdOx1 nCoV-19 vaccine (AZD1222) against SARS-CoV-2: an interim analysis of four randomised controlled trials in Brazil, South Africa, and the UK. *Lancet 397* (10269), 99−111.

(17) Baden, L. R., El Sahly, H. M., Essink, B., Kotloff, K., Frey, S., Novak, R., Diemert, D., Spector, S. A., Rouphael, N., Creech, C. B., et al. (2021) Efficacy and Safety of the mRNA-1273 SARS-CoV-2 Vaccine. *N. Engl. J. Med. 384* (5), 403−416.

(18) Lan, J., Ge, J., Yu, J., Shan, S., Zhou, H., Fan, S., Zhang, Q., Shi, X., Wang, Q., Zhang, L., et al. (2020) Structure of the SARS-CoV-2 spike receptor-binding domain bound to the ACE2 receptor. *Nature 581* (7807), 215−220.

(19) Shang, J., Wan, Y., Luo, C., Ye, G., Geng, Q., Auerbach, A., and Li, F. (2020) Cell entry mechanisms of SARS-CoV-2. *Proc. Natl. Acad. Sci. U. S. A. 117* (21), 11727−11734.

(20) Shang, J., Ye, G., Shi, K., Wan, Y., Luo, C., Aihara, H., Geng, Q., Auerbach, A., and Li, F. (2020) Structural basis of receptor recognition by SARS-CoV-2. *Nature 581* (7807), 221−224.

(21) Wang, Q., Zhang, Y., Wu, L., Niu, S., Song, C., Zhang, Z., Lu, G., Qiao, C., Hu, Y., Yuen, K. Y., et al. (2020) Structural and Functional Basis of SARS-CoV-2 Entry by Using Human ACE2. *Cell 181* (4), 894−904. e9.

(22) Jiang, S., Hillyer, C., and Du, L. (2020) Neutralizing Antibodies against SARS-CoV-2 and Other Human Coronaviruses. *Trends Immunol. 41* (5), 355−359.

(23) Rogers, T. F., Zhao, F., Huang, D., Beutler, N., Burns, A., He, W. T., Limbo, O., Smith, C., Song, G., Woehl, J., et al. (2020) Isolation of potent SARS-CoV-2 neutralizing antibodies and protection from disease in a small animal model. *Science 369* (6506), 956−963.

(24) Ju, B., Zhang, Q., Ge, J., Wang, R., Sun, J., Ge, X., Yu, J., Shan, S., Zhou, B., Song, S., et al. (2020) Human neutralizing antibodies elicited by SARS-CoV-2 infection. *Nature 584* (7819), 115−119.

(25) Huang, W. C., Zhou, S., He, X., Chiem, K., Mabrouk, M. T., Nissly, R. H., Bird, I. M., Strauss, M., Sambhara, S., Ortega, J., et al. (2020) SARS-CoV-2 RBD Neutralizing Antibody Induction is Enhanced by Particulate Vaccination. *Adv. Mater. 32* (50), 2005637.

(26) Yang, J., Wang, W., Chen, Z., Lu, S., Yang, F., Bi, Z., Bao, L., Mo, F., Li, X., Huang, Y., et al. (2020) A vaccine targeting the RBD of the S protein of SARS-CoV-2 induces protective immunity. *Nature 586* (7830), 572−577.

(27) Kanekiyo, M., Wei, C. J., Yassine, H. M., McTamney, P. M., Boyington, J. C., Whittle, J. R., Rao, S. S., Kong, W. P., Wang, L., and Nabel, G. J. (2013) Self-assembling influenza nanoparticle vaccines elicit broadly neutralizing H1N1 antibodies. *Nature 499* (7456), 102−6.

https://doi.org/10.1021/acs.bioconjchem.1c00208
Bioconjugate Chem. 2021, 32, 1034−1046

(28) Cho, K. J., Shin, H. J., Lee, J. H., Kim, K. J., Park, S. S., Lee, Y., Lee, C., Park, S. S., and Kim, K. H. (2009) The crystal structure of ferritin from Helicobacter pylori reveals unusual conformational changes for iron uptake. *J. Mol. Biol. 390* (1), 83−98.
(29) Kanekiyo, M., Bu, W., Joyce, M. G., Meng, G., Whittle, J. R., Baxa, U., Yamamoto, T., Narpala, S., Todd, J. P., Rao, S. S., et al. (2015) Rational Design of an Epstein-Barr Virus Vaccine Targeting the Receptor-Binding Site. *Cell 162* (5), 1090−100.
(30) Ma, X., Zou, F., Yu, F., Li, R., Yuan, Y., Zhang, Y., Zhang, X., Deng, J., Chen, T., Song, Z., et al. (2020) Nanoparticle Vaccines Based on the Receptor Binding Domain (RBD) and Heptad Repeat (HR) of SARS-CoV-2 Elicit Robust Protective Immune Responses. *Immunity 53* (6), 1315−1330. e9.
(31) Qi, M., Zhang, X. E., Sun, X., Zhang, X., Yao, Y., Liu, S., Chen, Z., Li, W., Zhang, Z., Chen, J., et al. (2018) Intranasal Nanovaccine Confers Homo- and Hetero-Subtypic Influenza Protection. *Small 14* (13), 1703207.
(32) Kang, Y. F., Sun, C., Zhuang, Z., Yuan, R. Y., Zheng, Q., Li, J. P., Zhou, P. P., Chen, X. C., Liu, Z., Zhang, X., et al. (2021) Rapid Development of SARS-CoV-2 Spike Protein Receptor-Binding Domain Self-Assembled Nanoparticle Vaccine Candidates. *ACS Nano 15*, 2738.
(33) Leung, K., Shum, M. H., Leung, G. M., Lam, T. T., and Wu, J. T. (2021) Early transmissibility assessment of the N501Y mutant strains of SARS-CoV-2 in the United Kingdom, October to November 2020. *Euro. Surveill. 26* (1), 2002106.

https://doi.org/10.1021/acs.bioconjchem.1c00208
Bioconjugate Chem. 2021, 32, 1034−1046